Chem. Rev. **1987**, *87*, 101–112

Chemical Dynamics and Kinetics Phenomena as Revealed by Sensitivity Analysis Techniques

HERSCHEL RABITZ

Princeton University, Department of Chemistry, Princeton, New Jersey 08544

Received June 2, 1986 (Revised Manuscript Received October 30, 1986)

Contents

I. Introduction and Background

Chemical phenomena may be conveniently divided into classes characterized as being microscopic or macroscopic in nature. In the former case, the first issue of concern involves atomic and molecular electronic structure and its manifestations in terms of spectroscopy and chemical behavior. At the other extreme are bulk static and kinetic phenomena involving macroscopic samples of matter. With these considerations in mind the natural hierarchical flow shown in Figure 1 may be considered. The connection between each of the levels or steps in the diagram involves complex chemical coupling processes represented by a solution of an appropriate chemical equation. For example, Schroedinger's equation would be utilized in relating the intermolecular potential to microscopic observables in a collision dynamics problem. The information available at each level of the flow in Figure 1 may be typically expressed by appropriate functions (e.g., a potential is usually presented as a function of coordinates, cross sections are a function of energy, rate constants are a function of temperature, concentrations are a function of position or time, etc.). The physical content at each level of the flow in Figure 1 is embodied in the shape and structure of these functions. The basic issue addressed by the sensitivity techniques presented in this paper concerns the relationship between the functions at each level of the flowchart.

A number of reviews have recently been written on the topic of sensitivity analysis[1-5] and these articles have generally emphasized an overview of the current literature. The present review intends to satisfy a different role by: (1) emphasizing the *function* relationships mentioned above, and (2) stressing the current directions of the field. In keeping with the goals here, specific numerical techniques will not be discussed. The numerical technology has matured to the level such that an examination of the types of problems and questions open for study is most appropriate at this time.

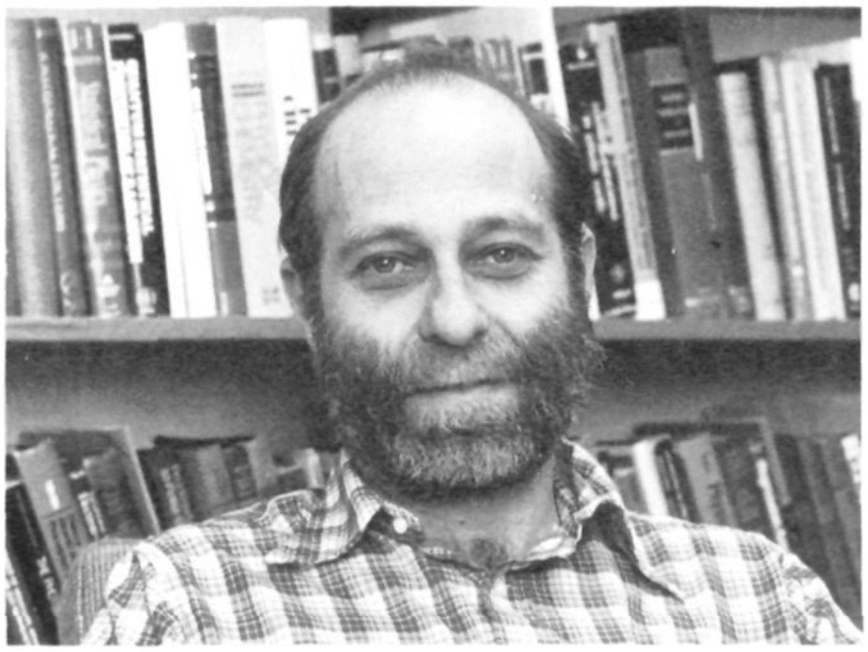

The author received his Bachelor's Degree in Chemistry from the University of California, Berkeley, in 1966. He then received a Ph.D. in Chemical Physics from Harvard University in 1970 and spent a postdoctoral year at the University of Wisconsin. From 1971 to the present time, he has been on the faculty of Princeton University. In 1975–1979 he was awarded an Alfred P. Sloan Fellowship, and in 1974–1979 he received the Camille and Henry Dreyfus Teacher–Scholar Award. Currently, he is a Professor of Chemistry and an Associate faculty member in the Program in Applied and Computational Mathematics at Princeton. Professor Rabitz's research interests are mainly in the area of chemical physics with an emphasis on molecular dynamics and chemical kinetics phenomena.

In order to better understand the context of the techniques presented in the subsequent sections, it is useful to consider the flowchart in Figure 1 from both a theoretical and an experimental perspective. First, the theoretical approach to dynamics or kinetics phenomena would naturally proceed from the left of Figure 1 through the hierarchy of possible observables in the laboratory. Although theoretical calculations are often employed to "compare" with laboratory data, theory has another useful, if not more important, role to play in gaining insight into the fundamental physical processes. In particular, when a class of observables has been calculated the fundamental questions still remains with regard to the relation between the observables and structure in the underlying dynamic or kinetic model. For example, the degree to which particular steps in a chemical mechanism control observable concentrations is an important issue in chemical kinetics. Questions

0009-2665/87/0787-0101$06.50/0

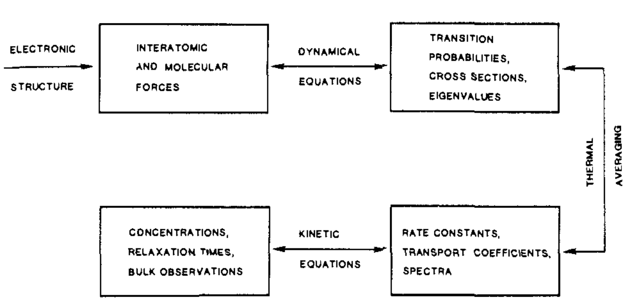

Figure 1. Flowchart illustrating the hierarchical connection between microscopic and macroscopic variables in chemical dynamics and kinetics. Sensitivity analysis techniques may be developed to specifically probe the parametric and functional interconnections between each of the levels of the flowchart. The double-headed arrows connecting elements in the flowchart imply that both *forward* and *inverse* questions may be explored.

of this type may be raised at all levels in the flowchart of Figure 1 when proceeding in the *forward* direction. Questions regarding the physical role of the input structure may be raised regardless of whether an approximate or an "exact" set of input is involved. When the model is employed to simulate a particular physical system, then a related question arises concerning how errors in the model propagate through to produce uncertainties in the calculated observables. This inherently statistical question and the previous issue about the role of model structure are physically distinct questions, although they may be approached by a common set of mathematical techniques. Each issue has its own realm of applicability, but the present review will primarily focus on tools for establishing the physical role played by structure in a model regardless of whether it is exact or approximate.

The questions raised in the previous paragraph may be reversed when considering the performance of actual experiments in a laboratory. From an experimental perspective, the input is on the right of the flowchart in Figure 1 and the goal is to extract more fundamental information residing on the left of the chart from the data. Such a process entails an inversion of the laboratory data and a host of issues may be immediately raised in this circumstance. Real laboratory experiments will be typically incomplete with regard to their information content for inversion to one or another level of the *inverse* flowchart and the data will also often be contaminated with noise. The techniques discussed in this review could in principle be employed in an actual inversion algorithm, but at this stage they seem to have a more basic use for gaining insight into the process of experimental design. In particular, it will be shown how to manipulate theoretical knowledge about the *forward* relationships in the flowchart to gain information about the utility of a given body of data for a possible inversion. It is in this context that theory will be used to explore both the forward and inverse questions involved in the structure–function relationships in chemical dynamics and kinetics.

Regardless of whether forward or inverse problems are of concern in the flowchart the basic operation necessary is to relate the functional form at one level of the flow to that at another level. This relationship is best understood by considering an example. The laboratory observable $\mathcal{O}(\rho)$ is taken as a function of a continuous variable ρ which could be the energy in the case of cross sections, temperature in the case of rate constants, time in the case of concentrations, etc. (ρ could also include discrete variables such as quantum indices, labeling state-to-state transitions). Taking the input to the model as residing at the microscopic dynamical level, the intermolecular potential function $V(\vec{r})$ controls the behavior of the observable. In most practical computations, the potential may actually be parameterized by fitting to some judicious functional form such that $V(\vec{r}) \rightarrow V(\vec{r},\alpha)$ where α is a vector of resultant parameters. In this case, a differential change in the observable would be related to a similar differential change in the parameters in the following fashion[1]

$$\mathrm{d}\mathcal{O}(\rho) = \sum_j \left[\frac{\partial \mathcal{O}(\rho)}{\partial \alpha_j}\right] \mathrm{d}\alpha_j \qquad (1)$$

where $\partial\mathcal{O}(\rho)/\partial\alpha_j$ is a sensitivity coefficient relating the observable at point ρ to a disturbance of the jth parameter. In the case of isothermal chemical kinetics where the rate constants are taken as model parameters, then the discrete variational form in eq 1 is quite appropriate. In this circumstance it is important to realize that the sensitivity coefficients $\partial\mathcal{O}(\rho)/\partial\alpha_j$ are physically the important quantities to examine and no explicit differential changes $\mathrm{d}\alpha_j$ in the parameters would actually be made.

The perspective implied by eq 1 is satisfactory if the underlying model is truly parametrically defined which is often the situation in chemical kinetics. However, for the case that was originally discussed in the previous paragraph, the intermolecular potential is actually a function in coordinate space despite the fact that it may be parameterized in numerical computations. Therefore, it is physically more constructive to treat the input as a function and consider the functional analogue of eq 1

$$\delta\mathcal{O}(\rho) = \int \left[\frac{\delta\mathcal{O}(\rho)}{\delta V(\vec{r})}\right] \delta V(\vec{r})\, \mathrm{d}\vec{r} \qquad (2)$$

where $\delta\mathcal{O}(\rho)/\delta V(\vec{r})$ is referred to as a *forward* functional sensitivity coefficient rating the observable $\mathcal{O}(\rho)$ at point ρ to a disturbance of the potential $V(\vec{r})$ at point $\vec{r}$. As a formulation of first order functional perterbation theory, eq 2 would be applied if a specific potential variation $\delta V(\vec{r})$ were made available for performance of the integral. In accord with eq 1, the emphasis is not on such an explicit implementation but rather on the examination of the forward sensitivity coefficients $\delta\mathcal{O}(\rho)/\delta V(\vec{r})$ constituting the kernel of the integral in eq 2. These coefficients act as the propagator of any arbitrary infintesimal disturbance $\delta V(\vec{r})$ through to the response $\delta\mathcal{O}(\rho)$ of the observable. The functional sensitivities may also be thought of as filters in that they take a projection of the input disturbance implied by eq 2 in order to produce a response on the observable. In summary, regardless of whether partial derivatives sensitivity coefficients or functional derivative sensitivity coefficients are examined, their ultimate physical meaning is best understood by reference to their roles in eq 1 and 2, respectively. At this stage it is not necessary to examine how the sensitivities are calculated; their physical role is the point being emphasized now.

In order to understand the inverse perspective introduced above, we may first recognize that eq 1 and

2 imply that the observable (or generally a set of them $\mathcal{O}_1(\rho),\mathcal{O}_2(\rho),...$) constitutes the original set of dependent variables while the parameter vector α or the function $V(\vec{r})$ (other functions would arise if input was considered at levels other than the hamiltonian) constitutes the set of independent variables. In consideration of inverse problems, this relationship is reversed and expressions analogous to eq 1 and 2 may now be produced

$$\delta\alpha_j = \int \left[\frac{\delta\alpha_j}{\delta\mathcal{O}(\rho)} \right] \delta\mathcal{O}(\rho)\ d\rho \tag{3}$$

$$\delta V(\vec{r}) = \int \left[\frac{\delta V(\vec{r})}{\delta\mathcal{O}(\rho)} \right] \delta\mathcal{O}(\rho)\ d\rho \tag{4}$$

Note that when considering the inverse for the discrete parameter case in eq 3, a functional relationship exists necessitating the calculation of inverse functional sensitivity coefficients $\delta\alpha_j/\delta\mathcal{O}(\rho)$ relating a disturbance in the observable at point ρ to a response of the parameter α_j. The inverse functional derivative $\delta V(\vec{r})/\delta\mathcal{O}(\rho)$ has a similar interpretation explicitly relating the observable function to the underlying model function. As with eq 1 and 2 the physical focus is on the kernals of eq 3 and 4 rather than the explicit introduction of disturbances in the observables. The latter issue would of course arise in the actual implementation of inverting real laboratory data which is not the focus in this paper.

A variety of other relations similar to eq 1–4 may be produced by exchanging different sets of dependent and independent variables, and some of these cases will be considered within the context of the particular applications below. In general the thrust of the remainder of this paper focuses on the interpretation and utility of various types of sensitivity coefficients for physically *understanding* relations between components in a model and various types of observables. In keeping with this aim section II will be concerned with collision dynamics and section III with chemical kinetics. Finally, section IV will present some concluding remarks particularly associated with the future directions of the subject.

II. Potential Structure and Chemical Dynamics

In principle, at the microscopic scale forward and inverse analysis would entail questions involving electronic structure, inter- or intramolecular forces, and microscopic observables such as collision cross sections and molecular spectral properties. Thus far, in practice the first of these steps involving electronic structure has not been systematically probed with these techniques, and we shall therefore focus on the relationship between inter- and intramolecular forces and appropriate microscopic observables. The remainder of this section is divided into two parts according to whether inter- or intramolecular processes are of concern.

A. Intermolecular Dynamics

The three classes of physical problems to be explored in this category involve elastic, inelastic, and reactive scattering. An emphasis will be placed on functional considerations since they provide the deepest insight into the fundamental processes.

1. Elastic Scattering

Although elastic scattering is sometimes considered an overworked area in chemical physics, there is still much to be learned with regard to mapping out the relationship between potential structure and behavior of the cross sections as a function of energy or scattering angle. This point may be best illustrated by considering the case of two idealized rare gas atoms interacting with a strictly repulsive potential.[6] A choice of potential is necessary in order to carry out the forward analysis of the problem and a model such as this provides a convenient testing ground for the basic ideas. To simplify the matter even further, consider only the integrated total cross section $\sigma(E)$ as a function of energy E. Even in this simple case surprising behavior can be found. To set the stage, first observe that on *classical* intuitive grounds one would expect $\delta\sigma(E)/\delta V(r) \geqslant 0$, since an arbitrary positive variation $\delta V(r) \geqslant 0$ of the purely repulsive potential would be expected to produce a concomitant positive response $\delta\sigma(E) \geqslant 0$ of the cross sections as embodied in eq 5. Before considering the validity of this supposition regarding the functional sensitivity in the integrand of eq 5, we must address a means of calculating the sensitivity coefficients.

$$\delta\sigma(E) = \int \left[\frac{\delta\sigma(E)}{\delta V(r)} \right] \delta V(r)\ dr \tag{5}$$

The general route to cross-section sensitivity information would be through the sensitivity of the scattering matrix elements or in this case just the phase shifts. However, for the case of the total cross section, the functional variation of the optical theorem may be explicity carried out to give the remarkably simple result[6,7]

$$\frac{\delta\sigma(E)}{\delta V(\vec{r})} = -\frac{16\pi^3\mu\hbar}{k}\ Im[\psi_{\vec{k}}(\vec{r})\psi_{-\vec{k}}{}^*(\vec{r})] \tag{6}$$

where the wave functions satisfy incident plane wave boundary conditions and μ is the collisional reduced mass. This expression provides a computationally practical means for obtaining the functional sensitivity on the left-hand side of eq 6 as well as establishing a clear physical interpretation for scattering wave functions. The latter point follows since the functional derivative itself has unambiguous physical meaning. In this context, it is interesting to note that scattering wave functions have received relatively little attention in dynamics which is in considerable contrast to the attention focused on bound-state wave functions, particularly in electronic structure problems.

Returning again to the scattering of two particles with a purely repulsive potential, we find in Figure 2 a plot of the resultant forward sensitivity surface.[6] At very short range the surface approaches zero implying quite naturally that potential variations in the deep tunneling region will have no effect on the observed cross section. In general, the surface is positive as intuitively argued above on classical grounds but a distinct negative trough appears as the first structure upon leaving the repulsive region. This unexpected negative region results from a complex quantum interference process implying that simple intuition on the role of different regions of the potential can be misleading at times.

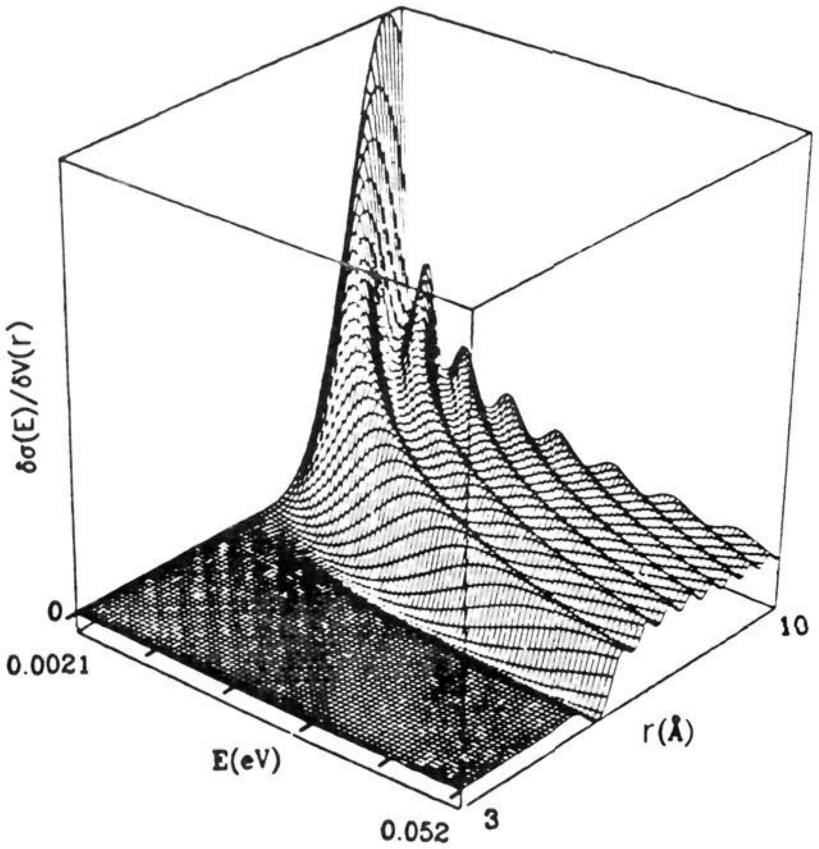

Figure 2. The forward functional sensitivity $\delta\sigma(E)/\delta V(r)$ (Å^{-1} eV^{-1}) for a model system represented by a purely repulsive, strictly symmetric interaction.[6] At a given energy, E, a cut through the surface is primarily a positive function with residual quantum oscillations. At sufficiently short range, the response surface goes to zero corresponding to the statement that the deep classically forbidden region has a small effect on the total elastic cross section. Given the repulsive nature of the reference potential, the negative trough apparent at short range is a surprise, implying that a further increase in the potential in this region would yield a decrease in the cross section.

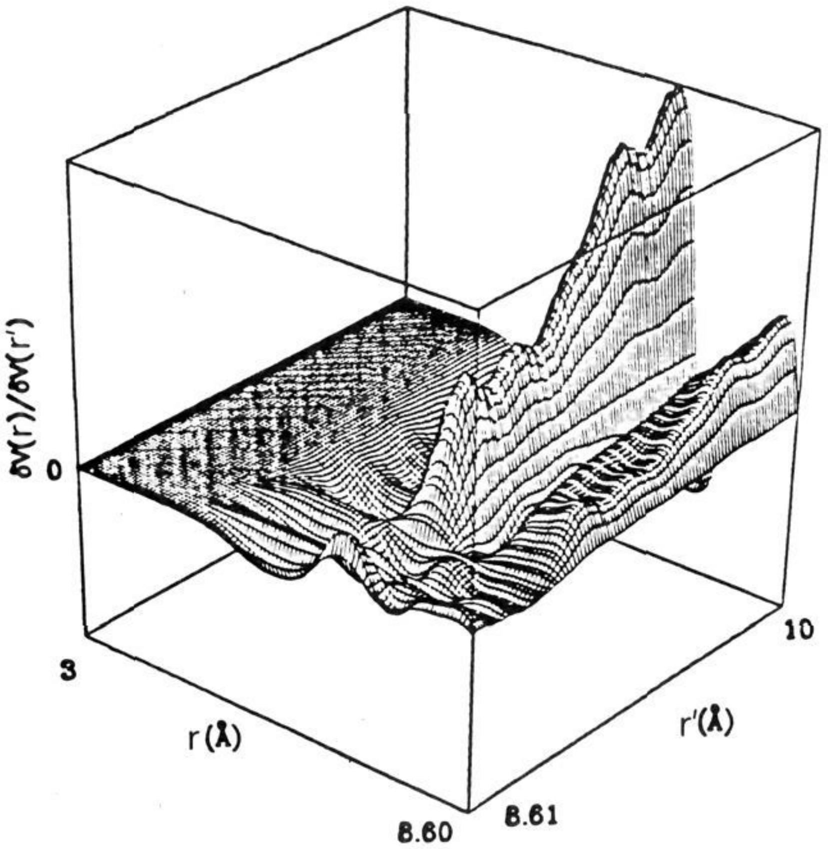

Figure 3. Correlation sensitivity coefficients $(\delta V(r)/\delta V(r'))_{\sigma(E)}$ with a subset of the total elastic cross sections constrained as fixed. The system corresponds to the elastic scattering of two particles described as having a spherically symmetric potential.[8] It is seen that a disturbance in the potential at long range may be compensated for by a similar disturbance in the same vicinity but at shorter range. However, as the point of compensation r moves to ever shorter range, the possibility for compensation is destroyed as evidenced by the correlation function going to zero.

As discussed in the introduction, forward surfaces such as in Figure 2 may be manipulated in various ways to glean additionally useful information. For example, an important physical question concerns whether a disturbance $\delta V(r)$ at a point r could be compensated for by a disturbance $\delta V(r')$ at a point r' so as to leave a given cross section $\sigma(E)$ invariant. Mathematically, this relation would take on the form

$$\delta V(r') = \int_I \left[\frac{\delta V(r')}{\delta V(r)}\right]_{\sigma(E)} \delta V(r)\,\mathrm{d}r \qquad (7)$$

where the index I denotes the fact that the integration over r is on a restricted domain excluding the range spanned by the variable r'. Therefore, the nonzero regions of the correlation sensitivity coefficient $(\delta V(r')/\delta V(r))_{\sigma(E)}$ as a function of r and r' will define correlation and hence nonuniqueness of a potential with respect to a constant cross section $\sigma(E)$. The desired correlation sensitivity coefficient may be obtained by exchanging appropriate dependent and independent variables to arrive at the following integral equation which must be solved[8]

$$\int_{II} \left[\frac{\delta\sigma(E)}{\delta \mathrm{V}(r')}\right] \left[\frac{\delta V(r')}{\delta V(r)}\right]_{\sigma(E)} \mathrm{d}r' = -\left[\frac{\delta\sigma(E)}{\delta V(r)}\right] \qquad (8)$$

where the index II denotes the fact that the r' integration is over an appropriate domain excluding that of I. A calculation where domain II is in the long-range portion of the potential and domain I is at short range is shown in Figure 3. It is clear that a disturbance at long range cannot be compensated for by a concomitant disturbance in the short-range repulsive region. However, there is a clear range of positive correlation evident with a rather complex involved structure.

The result in Figure 3 may be thought of as a partial exchange or inversion of the forward scattering information. Directly useful insight may be gained into inverse scattering through the following logic. By starting with a given potential we obtain collision cross sections as well as the forward functional sensitivity coefficients $\delta\sigma(E)/\delta\sigma(r)$. Recall again that these latter coefficients give the response of the cross section due to a disturbance of the potential. With all this information available we may now address how the potential would respond about its nominal value due to disturbances in the cross section. This question is addressed by the inverse sensitivity coefficient $\delta V(r)/\delta\sigma(E)$ which should be interpreted as a kernel of an intergral having the same form as eq 4. The inverse sensitivity coefficient may be obtained by solving the following integral equation[6,8]

$$\int \left[\frac{\delta\sigma(E)}{\delta V(r)}\right]\left[\frac{\delta V(r)}{\delta\sigma(E')}\right] \mathrm{d}r = \delta(E - E') \qquad (9)$$

where it is implicitly assumed that the forward kernel entering into eq 9 is invertable (at least as a generalized inverse). Equation 9 has a simple interpretation of an orthogonality relation between the forward and inverse sensitivity response surfaces. From this perspective a certain degree of qualitative insight into the inverse surface may be identified by a simple examination of the forward surface. In particular, for the essentially positive forward surface in Figure 2, it is apparent that the inverse surface must oscillate rather rapidly in sign in order to maintain the orthogonality property of eq 9. As an illustration of this behavior, Figure 4 gives a cut through the inverse surface at high energy, and the high-frequency ringing structure is quite apparent.

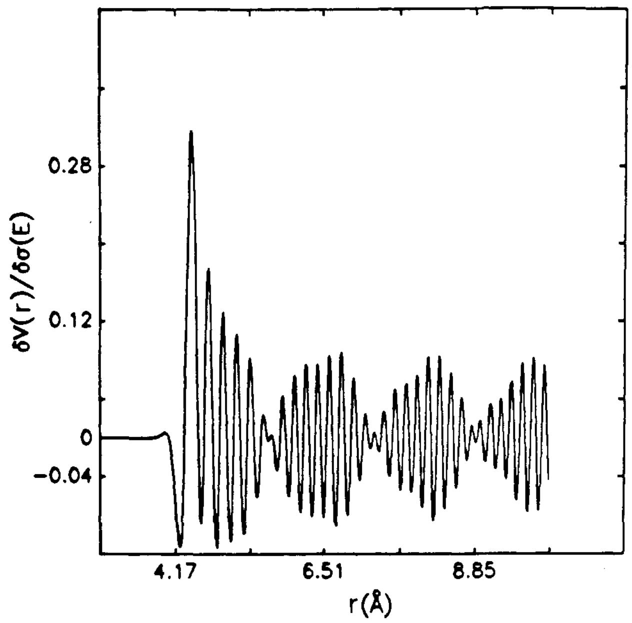

Figure 4. A cut through the inverse functional sensitivity surface $\delta V(r)/\delta\sigma(E)$ is a function of r at a high energy value E. This inverse sensitivity corresponds to the same system yielding the forward sensitivity surface in Figure 2.[6] One would expect a large positive response near the classical turning point and a null result at larger r values signifying little information being gained about the long-range tail of the potential. Quite surprisingly, this long-range behavior is not found with a rather symmetric high-frequency ringing pattern exhibited in the long-range region. The frequency and amplitude of these latter oscillations are quite sensitive to the energy and the intuitively expected result will be produced if a reasonable laboratory energy dispersion is folded in. It is apparent that a good quality measurement at high energy will yield information about the high-frequency components of the long-range part of the potential.

A simple analysis of Figure 4 provides some interesting insight into inverse atomic scattering. First, the primary utility of inverse information of this type resides in the fact that no parametric forms are involved in attaining this solution to what may be called the infinitesimal inverse scattering problem. This point is important since typical inversion algorithms will parameterize the potential and adjust the parameters until a reasonable fit to the data is obtained. Inherent in such a procedure is a potentially serious loss of flexibility through the constraint of choosing a particular functional form. Figure 4 clearly illustrates that unconstrained inverses can have a far more complex structure than would be intuitively expected. The present case is at high energy where the expectation is that knowledge about the potential near the classical turning point could be deduced.[9] The origins of this rule of thumb statement may be understood from Figure 4 when it is realized that the high-frequency beat structure is very sensitive to the energy and typical laboratory data involving a dispersion in energy would easily wash out any information at long range. In such a case, all that would remain is the dominant positive pulse and its small negative side component near the classical turning-point region. Although this latter negative feature is also unexpected, the overall dominant positive response would remain in accord with general expectations. A similar analysis at low energy reveals that the primary information about the potential is gained in its long-range portion, but again the results are somewhat surprising in that the inverse function is not uniform in that region.

Although only integrated cross sections were considered here, a rich amount of structure was evident in the various sensitivity surfaces. More structure will be apparent if differential cross sections are examined. If the actual potential has a typically attractive and repulsive well, additional interferences can also arise. These illustrations clearly serve to show that even in the well studied case of elastic scattering, there is much useful further information to be gained by examining functional response surfaces.

2. *Inelastic Scattering*

From the perspective being addressed here, the case of inelastic scattering introduces additional coordinate dependence into the potential function and quantum indices into the observable cross sections. A formula analogous to eq 6 may be derived again for the total cross section, but generally more useful results for state-to-state cross sections require the functional derivative of the scattering matrix $S_{\alpha\beta}$ where α and β denote appropriate initial and final states. The functional sensitivity of the scattering matrix has a very simple form in terms of the wave functions

$$\frac{\delta S_{\alpha\beta}}{\delta V(\vec{r})} = -2\pi i \psi^{\alpha}{}_{\vec{k}_\alpha}(\vec{r})\psi^{\beta *}{}_{-\vec{k}_\beta}(\vec{r}) \tag{10}$$

where $\vec{r}$ denotes all appropriate coordinates in the potential and the wave vectors are $\vec{k}_\alpha$ or $\vec{k}_\beta$. It is interesting to note that the product of wave functions in eq 10 consists of a wave impinging on the scattering center from the left and another from the right. As with the elastic case, this expression provides a practical means for computation as well as an explicit physical interpretation of the scattering wave functions.

Inelastic state-to-state forward functional sensitivity coefficients $\delta\sigma_{\alpha\beta}(E,\hat{\Omega})/\delta V(\vec{r})$ for scattering into solid angle $\hat{\Omega}$ can exhibit a considerable degree of variation as a function of all the involved continuous and discrete variables. Naturally, integration and summation over a portion of the variables would reduce this level of structure corresponding to the probing of less complex input–output questions. One interesting extreme limit of this process corresponds to the calculation of unit percent responses (UPR) which are defined as 100 × $\delta\sigma_{\alpha\beta}/\sigma_{\alpha\beta}$ where

$$100 \times \frac{\delta\sigma_{\alpha\beta}}{\sigma_{\alpha\beta}} = \int \left[\frac{\delta \ln \sigma_{\alpha\beta}}{\delta \ln V(\vec{r})}\right] d\vec{r} \tag{11}$$

The quantity 100 × $\delta\sigma_{\alpha\beta}/\sigma_{\alpha\beta}$ may be interpreted as the percentage response of the cross section $\sigma_{\alpha\beta}$ due to a unit percentage change in the potential V. A given UPR takes the entire sensitivity response surface as a function of $\vec{r}$ and reduces it to one characteristic number. A UPR number larger than unity implies that a disturbance of the potential will be magnified in the cross section. Table I presents UPR responses for the Ar–N_2 system at E = 0.032 eV by using the sudden approximation for the dynamics.[10] In this case, it is convenient to decompose the potential into the sum of an isotropic and anisotropic part. An expression exactly analogous to eq 11 may be written for the UPR for each of these two portions of the potential as presented in Table I. Two general comments are evident in the

TABLE I. State-to-State Rotationally Inelastic Differential Cross Section and Unit Percentage Response for Ar–N_2 at E = 0.032 eV

	$0 \rightarrow 2$	$0 \rightarrow 4$	$0 \rightarrow 6$	$0 \rightarrow 8$
cross section (θ = 10°)[a]	17.469	2.627	0.886	0.143
response[b]				
isotropic term	0.163	-8.507	-9.619	-8.932
anisotropic term	0.444	0.763	1.387	1.129
total	0.607	-7.744	-8.232	-7.803
cross section (θ = 60°)[a]	1.267	1.064	0.961	0.227
response[b]				
isotropic term	7.819	-0.838	-3.387	-5.508
anisotropic term	-2.260	-0.280	1.255	2.317
total	5.559	-1.118	-2.132	-3.191

[a] In units of Å^2 at scattering angle θ. Results are multiplied by 1000. [b] Calculated with $\delta\sigma_{0\rightarrow j}(\theta,E)/\delta \ln [V_{\text{isotropic}}(\vec{r})]$ and $\delta\sigma_{0\rightarrow j}(\theta,E)/\delta \ln [V_{\text{anisotropic}}(\vec{r})]$, respectively. This response may be interpreted as the percent change in the cross section per unit percent change in the potential.

table. First, the UPR values can be considerably larger than unity, corresponding to magnification of small disturbances in the potential. Second, the signs of the isotropic and anisotropic UPR number appear nearly random. In the case of the anisotropic term, logic based on perturbation theory alone would dictate a positive number, and this would appear to be the case for the higher order transitions. In general, the rather complicated sign dependence implies the existence of strong dynamical coupling. Strong coupling behavior can produce a severe scrambling of the role played by the potential or its components and only through direct sensitivity calculations can these roles be revealed.

All of the results discussed thus far have been based on treating the potential as a function in coordinate space. Other representations could just as well be considered, and to understand this point, it is best to realize that the potential is actually a continuous diagonal matrix in coordinate space $\langle \vec{r}|V|\vec{r}'\rangle = V(\vec{r})\delta(\vec{r} - \vec{r}')$. In practice, typical numerical calculations will be performed using a discrete quantum-state basis whereby the continuous matrix in coordinate space is replaced by its discrete analogue $\langle\alpha|V|\beta\rangle$ which will not be diagonal. The aggregate of elements corresponding to this discrete matrix may also be thought of as a surface, and similar input–output probings may be performed. A simple means of carrying out such an analysis would consist of replacing the potential matrix by a new matrix $\gamma_{\alpha\beta}\langle\alpha|V|\beta\rangle$ where the nominal value of $\gamma_{\alpha\beta}$ is unity for all α and β when performing the actual calculations. The introduction of the matrix γ conveniently allows for a probing of the contribution of any coupling matrix element. In terms of our "surfaces" a given coupling matrix element corresponds to a point on the discrete surface located with respect to its axes by the numbers α and β. All these notions may be put together to seek the pathway sensitivity coefficients which have the form

$$\left[\frac{\partial\sigma_{\alpha\beta}}{\partial\gamma_{rS}}\right]_{\gamma=1} \tag{12}$$

where the subscript implies that the gradient is evaluated at the nominal value of unity for each element in the γ matrix. The vibration–rotation inelastic scattering of He–HD was extensively explored with this pathway sensitivity technique.[11] Although the off diagonal vibrational matrix elements are typically small, leading to nearly perturbative vibrationally inelastic transitions, it was found that a given vibrationally inelastic cross section involved the participation of many rotationally inelastic coupling elements due to strong mixing amongst the states.

Finally, some inverse sensitivity coefficients have been calculated for inelastic scattering.[10] For the case of the Ar–N_2 system, it was found that inverting the total cross sections corresponding to those in Table I led to very little information regarding the potential. Much further exploration of forward and inverse inelastic scattering variation would be helpful at this point. Although quantum mechanical techniques were used in all the above illustrations, it would also be possible to raise the same questions utilizing classical mechanical dynamics. In this case, the first question to consider is whether features in the potential play essentially the same role in classical mechanics as they do in quantum mechanics. A preliminary examination of this topic has indicated an affirmative answer to the question; a severe exception occurs when extensive tunneling is involved.[12]

The elastic and inelastic calculations considered here have thus far been on a single adiabatic potential surface. When two adiabatic surfaces cross, the Born–Oppenheimer approximation can break down resulting in coupling between the surfaces. Therefore, a scattering system may enter on one surface and leave on another. The cross section for such an event will surely depend on the structure of the surfaces as well as the coupling terms between the surfaces. This matter then becomes a natural one to explore with functional sensitivity analysis techniques. As background, it is interesting to explore this same question within the framework of Landau–Zener theory for this process. This latter theory of atomic curve crossing focuses exclusively on the crossing point and therefore a functional variation analysis will be strictly local and show no sensitivity whatsoever to the potentials away from the crossing point. In reality a specific degree of breadth to the sensitivity will occur in the vicinity of the crossing point, and this issue was explored for a model of curve crossing in the He$^+$–Ne system.[13] Although quantum interference structure appeared in the results, they clearly show a discernable window of width ~0.2 Å about the crossing point.

3. *Reactive Scattering*

Thus far, little work has been carried out on using functional techniques to explore the input–output relations in reactive scattering. The formula in eq 10 also

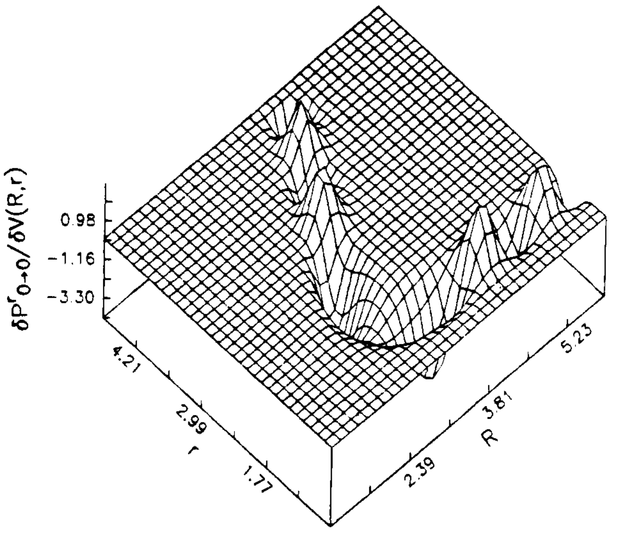

Figure 5. Functional derivative of the reactive transition probability $P^r_{0\to 0}$ with respect to a variation in the potential $V(r,R)$ for the collinear reaction of H + H_2.[14] The transition corresponds to the reactant and product molecules remaining in their ground vibrational states. The total energy is below the reactive barrier and the negative sensitivity in the barrier region the result of tunnelling being the reactive mechanism. Note that the strongest region of negative sensitivity occurs in the vicinity of the classical turning points symmetrically in the entrance and exit channels.

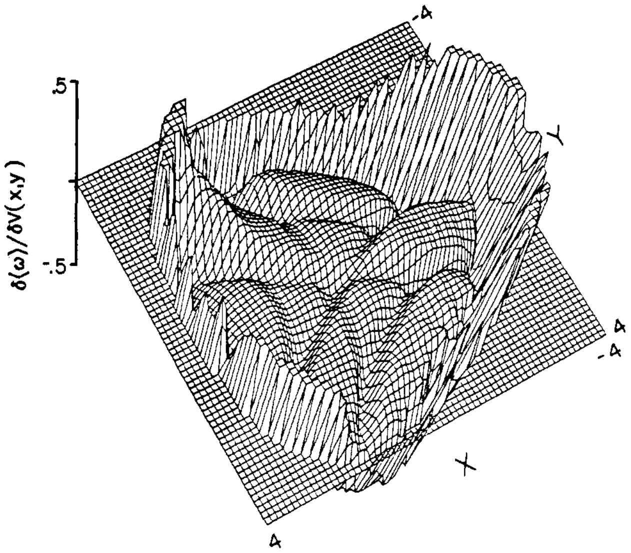

Figure 6. Functional sensitivity $\delta\langle\omega\rangle/\delta V(x,y)$ of the first moment $\langle\omega\rangle$ of the x-component of the frequency spectrum of a two-dimensional coupled anharmonic oscillator with respect to a variation of the potential $V(x,y)$. The calculation was performed by considering a single long-time projectory.[12] The high sensitivity near the outer boundaries of the traversed region is a result of the multitude of classical turning points in that region. In addition, a distinct pattern of sensitivity structure is apparent in the interior of the region corresponding to the trajectory caustics.

applies to the reactive case when α and β are interpreted to include channel indices as well as internal-state quantum numbers. It is also possible to consider an extension of eq 10 to treat variations in the unperturbed hamiltonian H_0 where the full hamiltonian has the form $H = H_0 + V$. Considerable care is needed in treating this latter case since variations in H_0 produce singular responses in the wave function through disturbances in the asymptotic boundary conditions.

The forward functional sensitivity analysis of the collinear reactive system $H + H_2(v) \rightarrow H_2(v') + H$, where v and v' are vibrational quantum numbers, has been extensively explored.[14] Figure 5 presents the functional sensitivity of the reactive transition probability $P^r_{0\to 0}$ while remaining in a ground vibrational state at an energy of $E = 0.403$ eV. This energy is below the reactive barrier, and chemical reaction only occurs due to tunneling. Thus, it is apparent that the reactive transition probability has a negative response to increases in the potential in the vicinity of the barrier. A detailed examination of the this figure shows that the most sensitive portion of the barrier is not at its maximum height but rather near the region of the classical turning points in the entrance and exit channels. At first sight this may seem to be surprising, but the result may also be analytically understood since the functional variation is proportional to products of incident wave functions from the entrance and exit channels in a fashion exactly analogous to the structure in eq 6. In general it was found that the sensitivity of the reactive transition probabilities to features in the potential surface can vary quite considerably as a function of energy. For example, at a resonance energy the structure of the response surface can differ quite substantially from that in Figure 5.

B. Intramolecular Processes

From a functional relationship point of view, inter- and intramolecular processes lead to very similar questions except the observables are now different. If chemical dissociation were to occur then the rate of this process would be an observable of natural concern in intramolecular dynamics. Even without reaction, the vibrational spectrum or its frequency moments may be measured in the laboratory. Both classical or quantum mechanical techniques may be utilized to explore the role of the intramolecular potential in controlling these observables. Realistic polyatomic molecules are currently restricted to classical techniques, and this situation will be considered here for illustration. The spectrum $I(\omega)$ is a function of the frequency ω and may be expressed as a Fourier transform of an appropriate coordinate correlation function.[15] Since the trajectory will be a functional of the intramolecular potential (in the case of classical mechanics, the functional dependence will extend only over the explicit regions of the surface sampled by the trajectories), the spectrum $I(\omega)$ will also be a functional of the potential. A similar statement would apply to the first moment $\langle\omega\rangle$ or higher moments of the spectrum. The sensitivity of the spectrum or its moments to structure in the intramolecular potential could be computed directly from knowledge of the functional derivative $\delta q(t)/\delta V(q')$ where $q(t)$ is an appropriate coordinate at time t and q' is a point on the potential surface. However, in the present circumstance where the observable is a functional of the trajectory $q(t)$ itself, then the considerably simplier technique of objective function sensitivity analysis may be applied.[12] This procedure is sometimes referred to as the adjoint technique,[16] and it may be applied in general to dynamics or kinetics problems when the actual observables represent a reduced set of information relative to the direct output from the model equations.

An example of the formulation discussed above is shown in Figure 6 for a model-coupled two-dimensional anharmonic oscillator where the anharmonic term has a cubic form.[12] The generally high degree of sensitivity to the intramolecular potential near the outer edges of the figure corresponds to regions of classical turning point density where the particle spends an extensive amount of time. In addition, the internal structure in the figure may be similarly associated with the caustics of the trajectory. The same techniques emphasized here could be used to explore systems in the chaotic regime provided that trajectories can be performed in a numerically reliable fashion.

III. Mechanistic Structure and the Behavior of Kinetic Systems

The type of questions being discussed in this review have been most extensively examined previously in the field of chemical kinetics.[2,3,5,17] Therefore no attempt will be made here to give an extensive review of the subject. Rather, an especially important general conclusion from a number of computational studies will be emphasized. In particular, it will be argued that the generally nonlinear nature of chemically kinetic systems under appropriate conditions can give rise to a dramatic simplification of the system response to any possible disturbances.[18] We will refer to these circumstances as producing scaling or self-similarity conditions. The examples cited below were especially chosen with this point in mind.

Given the flowchart in Figure 1, it is apparent that chemical concentrations and resultant thermodynamic variables could be explored with regard to their relation to structure at the atomic and molecular force field or potential level. Such an analysis has thus far not been carried out, and current kinetics work has focused on the phenomenological approach of starting with the chemical mechanism, perhaps including transport processes, and then proceeding to solve the appropriate model equations to yield chemical concentrations or other laboratory observables. This approach constitutes a forward analysis in parallel with the discussion in section II and thus far very little effort has been carried out regarding inverse questions with analogous sensitivity techniques.[19] Accordingly, only forward analysis issues will be treated here.

Although a functional approach to kinetic system analysis could be considered, it has been more traditional to treat these problems from a parametric point of view since the rate constants and transport coefficients are usually thought of as discrete parameters. Therefore, a natural quantity to explore would be the sensitivity coefficient $\partial C_i(r,t)/\partial \alpha_j$ providing the sensitivity of the ith the concentration at position r and time t with respect to a disturbance of the jth system parameter. The magnitude of these gradients provides a direct quantitiative measure of the significance of particular parameters with respect to the choosen concentrations. Even in these cases an important functional question still arises since in principal it is possible to introduce a disturbing flux $\delta J_n(r',t)$ of the nth chemical species and monitor the response of any other chemical species. This type of disturbance response is characterized by the elements of a square Green's function matrix

$$G_{in}(r,t;r',t') = \delta C_i(r,t)/\delta J_n(r',t') \qquad (13)$$

These latter functional derivatives may be shown to control the overall parametric sensitivity behavior of the gradients $\partial C_i(r,t)/\partial \alpha_j$ as well as to provide basic information about the stability of the chemical system. The method of computing parametric or functional sensitivity coefficients in kinetic problems has continued to evolve over the past several years and there is currently an emphasis on utilizing the available computational structure in solving the original model equations.

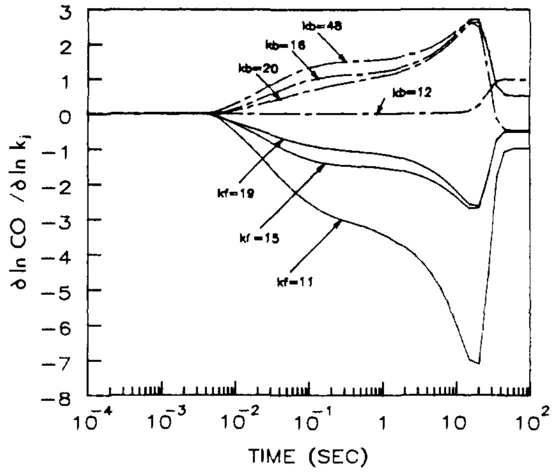

Figure 7. Rate constant sensitivity coefficients of carbon monoxide in a model system simulating the moist oxidation of carbon monoxide as a well stirred, purely temporal system.[17] Only a portion of the rate constant sensitivities are shown here for clarity; the curves are labeled by reaction steps in the mechanism (see ref 17). The most apparent feature in Figure 7 is the self-similarity between most of the curves as a function of time. Although each rate constant corresponds to a physically distinct step in the mechanism, their distinguishing role has become blurred due to kinetic coupling to produce the self-similar structure.

The remainder of this section is divided into four parts. The first three parts, A, B, and C, deal specifically with some illustrations respectively from time-dependent kinetics, steady-state kinetics including diffusive and convective terms, and space–time problems. Finally in section D the origin of the self-similarity and scaling behavior apparent in the previous three subsections will be discussed. Given the space limitations inherent in this article, there are a number of significant ancillary applications in kinetics which cannot be discussed here. The interested reader is referred to the literature for further information.[1-3,5,20]

A. Time-Dependent Kinetic Systems

The laboratory conditions of an isothermal well-stirred chemical reactor constitute perhaps the most common regime of study in chemical kinetics. In this situation the problem reduces to studying just the chemical kinetic steps since mass, momentum, and energy-transfer processes are eliminated from consideration. For such a reactor, the only parameters remaining are the rate constants and initial chemical concentrations. Although the latter parameters are distinct in that they may be controlled in the laboratory, both classes may be similarly addressed with regard to their control of the chemical kinetic system. Figure 7 illustrates some of the sensitivity coefficients for a model of the moist oxidation of carbon monoxide.[17] For the constants being probed in the mechanism, there is initially no sensitivity to those respective steps in the mechanism, but as time evolves, each has a distinct contribution to the carbon monoxide concentration at time t. At long times the sensitivity coefficients approach a constant corresponding to their role in establishing the equilibrium concentrations of the mixture. The most apparent feature in Figure 7 is the self-similarity between most of the curves as a function of time (i.e., there is a distinct relationship between the role of each of the rate constants reflecting itself in the curves approximately being multiples of one another). In a given system, including that of the present carbon monoxide oxidation problem, it is typically found that all of the rate constants do not produce self-similarity sensitivity behavior but a strong degree of correlation is often evident. The origin of this behavior will be discussed in section III.D.

The Green's function elements introduced in eq 13 have a very clear physical meaning for purely temporal kinetics. In this case the Green's function elements have the form $G_{in}(t,t') = \delta C_i(t)/\delta J_n(t') \equiv \partial C_i(t)/\partial C_n(t')$ such that they give the response of the ith concentration in time t to a disturbance of the nth concentration at time t'. This matrix thereby provides direct information on the stability of the system with regard to introduced chemical disturbances. This interpretation is important in its own right, but the matrix also controls all rate constant sensitivities since a disturbance of any rate constant will ultimately influence the chemistry through an alteration of the chemical concentrations. This statement may be mathematically established and has been utilized a number of times for practical computational purposes.[1] The eigenvalues of the Green's function matrix $G(t,t')$ may be thought of as stability or growth factors depending on whether their magnitude is less than or greater than unity, respectively. For example, the onset of a chemical explosion is indicated by one or more eigenvalues of the matrix being larger than unity in magnitude with greater values implying a more intense explosion. The physical content of these matrices could in principle be exploited for design purposes especially concerning the development of stable chemical systems, but this application has yet to be pursued in earnest.

If a given element $G_{in}(t,t')$ of the Green's function matrix is large, then the two chemical species involved, C_i and C_n, are "connected" through the evolutionary kinetics of the system. Knowledge of this linkage is physically important, but such indications do not in themselves explain the chemical *pathway* for the linkage. The chemical mechanism may give insight into this matter, but this input coupling structure alone will typically give a very incomplete picture if the reactive network involves strong chemical mixing. To address this question, a special class of reduced Green's function matrices $G^R(t,t')$ may be calculated to probe the pathways that chemical disturbances propagate.[21] For example, if species C_m is suspected of being an important linkage between C_i and C_n, then its role as an intermediary may be established by not allowing C_m to respond to any disturbance of C_n. A critical point to understand is that C_m is not actually removed from the chemical mechanism, but merely restricted to its nominal temporal trajectory.

B. Steady-State Premixed Systems

The steady-state analysis of the temporal problems in part III.A reduces to the study of a pure algebraic equation, and a well-known case involves the examination of chemical equilibrium properties. In this section our focus is not on this class of problems but rather steady-state problems where diffusion and reaction are both playing a role. A practical case of importance involves combustion in steady premixed flames.[22] In this situation the fuel and oxidizer are mixed behind the cold adiabatic boundary, and the flow rate is adjusted to match the flame speed to produce a steady system. This problem is also equivalent to transforming to a moving frame of reference at the flame speed in a steady propagating premixed system. Concentration gradients will typically develop due to the nonuniform evolution of the various species as a function of position in the flow. Sensitivity with respect to rate constants as well as diffusion coefficients may be explored in these cases. Diffusion is typically found to be important especially for species of small mass. In addition the presence of both upstream and downstream boundary conditions opens up these conditions for sensitivity probing. In general, the role of any parameter or external condition in such a problem may be explored for its contribution in controlling the chemistry.[23]

The role played by diffusion is an especially important question, since it is the first transport term going beyond the case of a well-stirred reactor. The Green's function elements provide a particularly simple means to explore this question. This comment may be understood by first realizing that an element of the purely temporal Green's function matrix $G_{in}(t,t')$ is strictly zero for $t' < t$ due to reasons of causality. On the other hand for the analogous steady-state one-dimensional problem, the Green's function matrix element $G_{in}(x,x')$ has no such restriction since diffusion may carry material upstream in the flow. Therefore, a comparision of $G_{in}(t,t')$ and $G_{in}(x,x')$ for two analogous systems with the same chemistry provides a direct measure of the role of diffusion by examining the region $x' > x$. Figure 8, parts a and b, respectively, shows elements of the Green's function matrix establishing the sensitivity of CO_2 to a disturbance of H_2 for a system corresponding to the moist oxidation of CO in the pure temporal limit and for the case of steady premixed flame.[21] The qualitative structure of the two Green's function plots is similar except for the pronounced region of sensitivity for $x' > x$ in the case of Figure 8b which is a result of diffusion playing a significant role in this system. This circumstance is not surprising since hydrogen has such a small mass and will easily diffuse. The presence of diffusive processes may alter the chemical pathways and make certain reactions more important than would otherwise be expected.

C. Unsteady Systems

The modelling of chemical kinetic systems involving spatial inhomogenieties as well as temporal evolution is a formidable task in itself.[24] Problems such as these have been most successfully explored at a practical level in atmospheric chemistry and combustion phenomena. The calculation of sensitivity information may proceed along the lines discussed in sections III.A and III.B above. Although only a limited number of sensitivity calculations have been carried out in problems of this

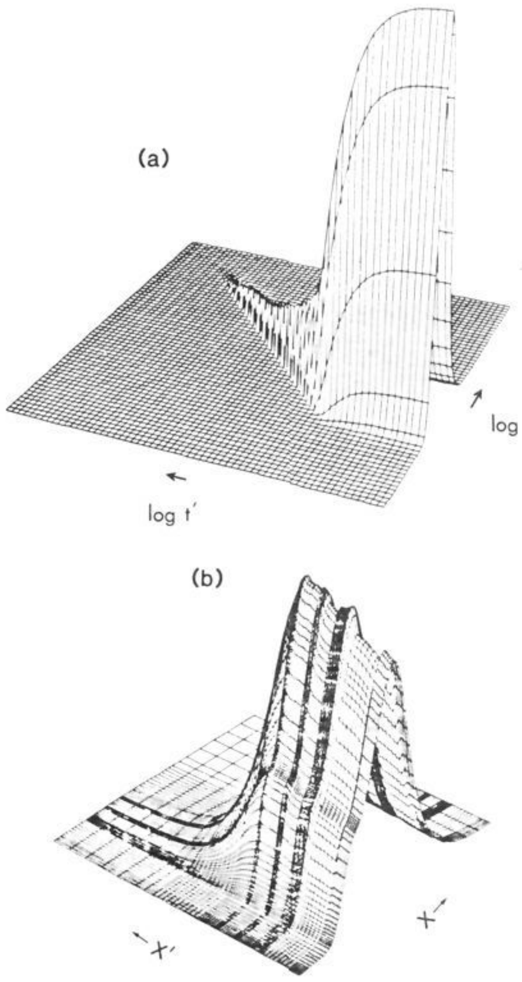

Figure 8. A sensitivity of carbon dioxide with respect to a disturbance of the flux of hydrogen. (a) The purely temporal case of a well-stirred reactor[17] where it is apparent that causality demands that the response of carbon monoxide at time t is strictly restricted to nonzero values only for $t > t'$. (b) The case of a steady premixed flame in one dimension[21], where the presence of diffusion is clearly indicated by the response of carbon monoxide at position x upstream, $x < x'$, in the flow. A comparison of Figures a and b gives an explicit measure of the role of diffusion.

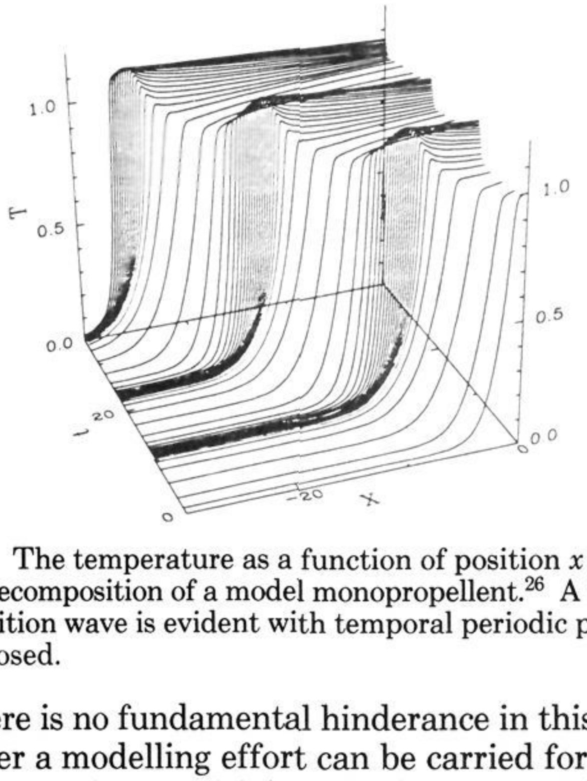

Figure 9. The temperature as a function of position x and time t for the decomposition of a model monopropellent.[26] A travelling decomposition wave is evident with temporal periodic pulsations superimposed.

type, there is no fundamental hinderance in this regard. Whenever a modelling effort can be carried forth, then an accompanying sensitivity calculation would also be most valuable for establishing which components and parameters in the model are physically significant.

A simple system providing useful insight is that of a propagating–pulsating flame produced by the chemical decomposition of an idealized monopropellant.[25] Figure 9 shows the temperature as a function of position and time with the presence of periodic temporal pulsations clearly evident on the flame front and in the post flame region. The pulsations result from an instability driven by the difference between the mass and thermal diffusivity coefficients. The temperature (and

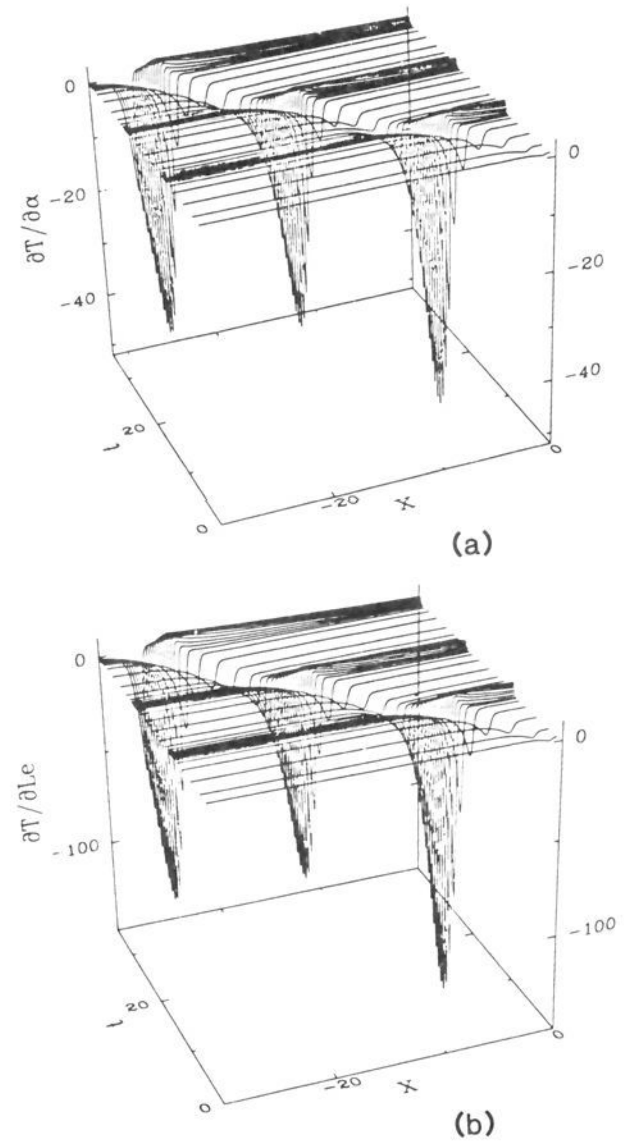

Figure 10. The temperature sensitivity with respect to the rate constant α (a) and Lewis number L_e (b) for the same model system depicted in Figure 9. Self-similarity is clearly evident in the temporal and spatical response of these two distinctly different parameters.

species) in a problem like this has an apparent dependence on position x and time t in the following fashion

$$T = T(x + vt,\ t/\tau, \alpha) \qquad (14)$$

where v is the flow velocity associated with overall movement of the front, and the vector α includes all appropriate kinetic and transport parameters. The extra time dependence embodied in t/τ describes the periodic pulsing where τ is the time period. Figure 10 gives the sensitivity to the rate constant and Lewis number, and a clearly distinct pulse structure is apparent.[26] This behavior may be understood from a sensitivity analysis of the general form of eq 14. In addition, a clear degree of self-similarity exists between the two plots in Figure 10 and this type of behavior is again reminiscent of what was found in Figure 7. An explanation for this self-similarity will be given in section III.D below. The velocity v and the period τ depend on the system parameters α and the role that these parameters play may be established by calculating $\partial v/\partial \alpha_i$ and $\partial \tau/\partial \alpha_i$. The calculation of these latter quantities is a straightforward matter and in general any characteristic parameter evident in the observables may be probed for its connection to details in the underlying model.

D. Self-Similarity and Scaling Behavior in Kinetic Systems[18]

The equations of chemical kinetics are typically nonlinear through both the reactive rate processes as well as possibly the additional conservation equations. The presence of nonlinearity is well-known to be capable of producing unusual behavior including limit cycles, chemical explosions, bifurcation phenomena, etc. In addition, the mathematical equations are not as amenable to the type of analysis that may be applied to linear equations such as in quantum mechanics. The behavior of linear systems is restricted to that admissible from linear superpositions of its fundamental solutions. With these comments in mind, it is unusual to see self-similarity structure arising frequently in kinetics problems as found, for example in Figures 7 and 10. While no evidence for this type of behavior has been found in quantum mechanical problems the possibly general existence of self-similarity and scaling behavior in kinetics systems is perhaps the most important general result to arise thus far from kinetic sensitivity analysis.

The existence of nonlinear structure in kinetic models can give rise to a situation where a single *dependent* variable, or perhaps a small subset of them, has a dominant controlling role in the physical mechanism. An example of this situation is the temperature in a flame system or perhaps a critical radical in other cases. Assuming the existence of a single such critical dependent variable, we will take it to be the first member of the concentration set $C_1(x,\alpha)$ without any loss of generality. In addition for convenience the independent coordinate is denoted as x (time or other space–time variables could also be considered). The above arguments lead to the following ansatz

$$C_i(x,\alpha) \simeq F_i(C_1(x,\alpha)), \quad i \neq 1 \qquad (15)$$

where F_i is a function giving all of the x and α dependence through its argument $C_1(x,\alpha)$. Parameter controlling consequences immediately follow from eq 15, and it is a simple matter to derive the following self-similarity conditions for the parameter sensitivity coefficients

$$\left[\frac{\partial C_i}{\partial \alpha_j}\right] \simeq \left[\frac{\partial C_1}{\partial \alpha_j}\right]\left[\frac{\partial C_i}{\partial x}\right]\left[\frac{\partial C_1}{\partial x}\right]^{-1} \qquad (16)$$

and for the system Green's function

$$\left[\frac{\delta C_i(x)}{\delta J_n(x')}\right] \simeq \left[\frac{\delta C_1(x)}{\delta J_n(x')}\right]\left[\frac{\partial C_i}{\partial x}\right]\left[\frac{\partial C_1}{\partial x}\right]^{-1} \qquad (17)$$

The physical significance of these equations is immediately clear. For example, through eq 16 the sensitivity coefficients for all chemical species to all parameters may be directly expressed in terms of the sensitivities $\partial C_1/\partial \alpha_j$ of the critically dominant dependent variable combined with slope information about the kinetic profiles. A similar statement also applies to the system Green's functions. As an illustration of this point, Figure 11 presents the sensitivity coefficients of the temperature and hydrogen atom concentration with respect to the mass diffusivity coefficients in a hydrogen–air steady premixed flame.[27] The temperature is the dominant variable, and the self-similar structure of the hydrogen atom sensitivities follow eq 16 to a high degree of accuracy. It is also possible to go a step further and argue that the fundamental Green's function elements satisfy the relation

$$\delta C_i(x)/\delta J_n(x') \simeq \mathcal{C}_i(x) j_n(x') \qquad (18)$$

where $\mathcal{C}_i(x)$ and $j_n(x')$ prescribe the approximate separable nature of the Green's function. A combination of eq 16–18 leads to the following simple result for the sensitivity coefficients

$$\frac{\partial C_i(x)}{\partial \alpha_j} \simeq \lambda_i(x)\, \sigma_j$$

where

$$\lambda_i(x) = \mathcal{C}_i(x)\left[\frac{\partial C_i}{\partial x}\right]\left[\frac{\partial C_i}{\partial x}\right]^{-1} \qquad (19)$$

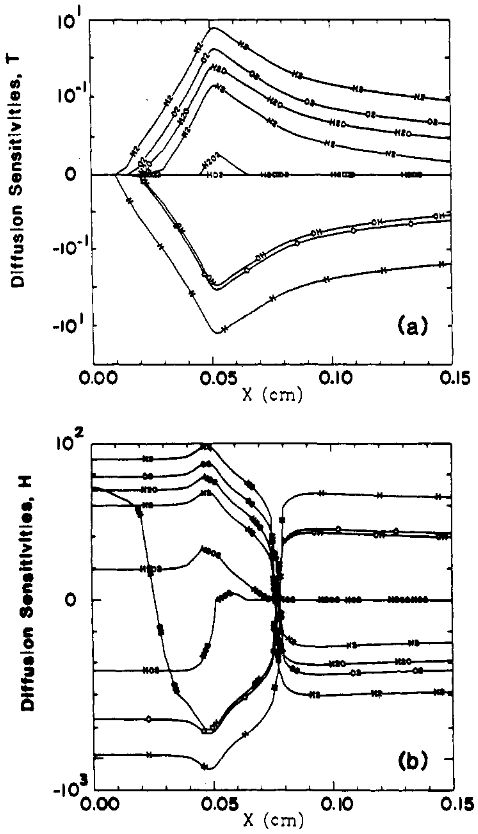

Figure 11. Temperature (a) and hydrogen atom (b) concentration sensitivity coefficients with respect to the mass diffusion coefficients D in a hydrogen–air steady, premixed flame. Each curve is labeled by the diffusion coefficient of a particular species. The temperature plays the role of a dominant, dependent variable through which all system disturbances primarily act. This role produces the strong self similarities between the sensitivity behavior in both plots (except for that of D_{OH}). The detailed behavior of the hydrogen atom sensitivity profiles closely follows the formula in eq 16.

The characteristic constants σ_j scale the sensitivity coefficients for a given dependent variable with respect to the various parameters. The sensitivities in Figures 7, 10, and 11 scale in this fashion. Another interesting conclusion follows from the fact that the Green's function elements in eq 18 are in principle measurable in the laboratory. In particular, the information on the right hand side of eq 18 could be measured. This implies that sensitivity coefficients, even those with respect to parameters not directly controllable in the laboratory, may be indirectly measured through a combination of eq 18 and 19 and appropriate laboratory experiments.

The degree of validity of eq 16–19 in any particular problem may be established by a simple examination of the sensitivity coefficients. In addition, an establishment of the critically dominant dependent variable may be definitively identified by consideration of the same type of reduced Green's functions introduced in section III.A. By constraining the spatial and/or temporal structure of C_1 to its nominal form, one may determine if it is indeed playing the critical role as the prime linkage for all system responses. In a constrained calculation of this type, all of the sensitivity structure would be radically different from that found without the constraints, thereby confirming that C_1 was the suspected dominant variable. The mathematical structure of the key ansatz in eq 15 is of the same form as that arising in central manifold theory[28] describing nonlinear system collapse at dynamical critical points. The essential difference here is that eq 15 has a broader context of validity. Finally, eq 15 implies that the typically many dependent variables describing the system may be reduced to knowledge of one (or a few) critical dependent variables, along with the functions F_i. The establishment of these latter functions may be a complex task in many cases.

IV. Concluding Comments

This paper has aimed to present a selected topical overview of how the relationship between model structure and observable behavior may be beneficially studied in chemical dynamics and kinetics. In the case of molecular dynamics, the new use of functional variations was emphasized rather than the more limited application of discrete parametric variations. For kinetics, parametric variations are still quite natural, and the present review emphasized the apparently broad existence of scaling and self-similarity conditions in strongly coupled kinetic systems. A number of specialized topics and applications were not discussed in this paper, and the reader is referred to other recent reviews[1-5] citing the available literature for further information. The techniques involved in probing the input–output relations are quite general and may be broadly applied to virtually any mathematical modelling problem. Indeed, there is parallel literature on this topic in a number of other areas of science and especially engineering.[29,30] The historical origin of systematic sensitivity analysis techniques lies primarily in the engineering disciplines, but the same basic tools have much to offer for solving centrally important problems in fundamental areas of chemistry and physics. The practical economics and safety aspects of large-scale engineering projects originally stimulated the development of these techniques in that area of application. Certainly the fundamental questions raised in the sciences make these tools of no less equal value!

The mathematical structure of sensitivity analysis, whether functional or parametric, parallels that of thermodynamics as a problem of multivariable analysis. Just as in thermodynamics, any physically meaningful question about a chemical model or its behavior may be addressed by one or another sensitivity coefficient (gradient). The cost of computing sensitivity information is diminishing rapidly as the available algorithms become more efficient; in many cases the overhead of performing sensitivity calculations is only a small fraction of the cost of evaluating the original model. Although there is considerable room for further development and elaboration of the basic tools and techniques, sophisticated applications can clearly be undertaken at this point with the result being unique insight into the inner workings of the physical problem. Currently in the case of kinetics and dynamics, an important practical goal is to combine both topics for forward and inverse analysis of the entire flowchart in Figure 1. For example, the degree to which bulk observables at the end of the chain retain information regarding the microscopic hamiltonian is still an issue with a paucity of understanding. In general the techniques presented in this paper will in themselves not solve physical problems, but they provide a powerful means of aiding in such an analysis.

Acknowledgments. I acknowledge the Department of Energy, The Office of Naval Research, and the Air Force Office of Scientific Research for supporting various aspects of my own research on the topic of this review.

References

(1) Rabitz, H.; Kramer, M.; Dacol, D. *Annu. Rev. Phys. Chem.* **1983**, *34*, 419.
(2) Tilden, J.; Costanza, V.; McRae, G.; Seinfeld, J. *Modelling of Chemical Reactions Systems*; Ebert, K., Deuflhard, P., Jager, W., Ed.; Springer-Verlag: Berlin, 1981; p 69.
(3) Rabitz, H. *Physica D*, in press.
(4) Eno, L.; Rabitz, H. *Adv. Chem. Phys.* **1982**, *51*, 177.
(5) Rabitz, H. *Comput. Chem.* **1981**, *5*, 167.
(6) Guzman, R.; Rabitz, H. *Chem. Phys.* **1986**, *109*, 85.
(7) Shi, S.; Rabitz, H., submitted for publication in *J. Chem. Phys.*
(8) Guzman, R.; Rabitz, H. *J. Chem. Phys.*, in press.
(9) Amdur, I.; Jordan, J. *Molecular Beams*; Ross, J., Ed.; Interscience: New York, 1966; Chapter 2.
(10) Guzman, R.; Rabitz, H. *J. Chem. Phys.*, in press.
(11) Kreutz, T.; Eno, L.; Rabitz, H., to be published.
(12) Judson, R.; Rabitz, H., submitted for publication in *J. Chem. Phys.*
(13) Mishra, M.; Rabitz, H., to be published.
(14) Shi, S.; Rabitz, H., submitted for publication in *J. Chem. Phys.*
(15) Noid, D.; Koszykowski, M.; Marcus, R. *J. Chem. Phys.* **1977**, *67*, 404.
(16) Lewins, J. *Importance - The Adjoint Function*; Pergamon: Oxford, 1965.
(17) Yetter, R.; Dryer, F.; Rabitz, H. *Combust. Flame* **1985**, *59*, 107.
(18) Rabitz, H.; Smooke, M., submitted for publication in *J. Phys. Chem.*
(19) Eno, L.; Beumee, J.; Rabitz, H. *Appl. Math. Comput.* **1985**, *16*, 153.
(20) Vajda, S.; Valko, P.; Turânyi, T. *Int. J. Chem. Kinet.* **1985**, *17*, 55.
(21) Mishra, M.; Peiperl, L.; Reuven, Y.; Rabitz, H.; Yetter, R.; Smooke, M., to be published.
(22) Glassman, I. *Combustion*; Academic: New York, 1977.
(23) Reuven, Y.; Smooke, M.; Rabitz, H. *J. Comput. Phys.* **1986**, *64*, 27.
(24) Lapidus, L.; Pinder, G. *Numerical Solution of Partial Differential Equations in Science and Engineering*; Wiley: New York, 1982.
(25) Smooke, M.; Koszykowski, M. *SIAM J. Sci. Stat. Comput.* **1986**, *7*, 301.
(26) Reuven, Y.; Rabitz, H.; Smooke, M., to be published.
(27) Reuven, Y.; Rabitz, H.; Smooke, M.; F. Dryen, submitted for publication in *Comb. Flame.*
(28) Hassard, B.; Wan, Y. *J. Math. Anal. Appl.* **1978**, *63*, 297.
Fernandaz, A.; Sinanoglu, O. *J. Math Phys.* **1984**, *25*, 2576.
(29) Tomovic, R.; Vukobratovic, M. *General Sensitivity Theory*; American Elsevier: New York, 1972.
(30) *Systems Sensitivity Analysis*; Cruz, J., Ed.; Dowden, Hutchison and Ross: Stroudsburg, PA, 1973.